Analyzing the PMIP4-CMIP6 ~~ensemble~~ collection: a workflow and tool (pmip_p2fvar_analyzer v1)

Anni Zhao[1], Chris M. Brierley[1], Zhiyi Jiang[1], Rachel Eyles[1], Damián Oyarzún[1], and Jose Gomez-Dans[1]

[1]Dept of Geography, University College London, London, WC1E 6BT, UK

Correspondence: Anni Zhao (anni.zhao.16@ucl.ac.uk)

Abstract. Experiment outputs are now available from the Coupled Model Intercomparison Project's 6th phase (CMIP6) and the past climate experiments defined in the Model Intercomparison Project's 4th phase (PMIP4). All of this output is freely available from the Earth System Grid Federation (ESGF). Yet there ~~are~~is overhead in analysing this resource that may prove complicated or prohibitive. Here we document the steps taken by ourselves to produce ensemble analyses covering past and future simulations. We outline the strategy used to curate, adjust the monthly calendar aggregation and process the information downloaded from the ESGF. The results of these steps were used to perform analysis for several of the initial publications arising from PMIP4. We provide post-processed fields for each simulation, such as climatologies and common measures of variability. Example scripts used to visualise and analyse these fields is provided for several important case studies.

1 Introduction

Paleoclimate modelling has long been used to understand the mechanisms of past climate changes, and also has served as a tool to test the response of climate models to the out-of-sample boundary conditions and forcings like high atmospheric CO_2 concentration that are used in future climate change projections (e.g. Harrison et al., 2014, 2015; Schmidt et al., 2014). Model intercomparison projects have become important in climate research, which run multiple models under the same identical experimental design that helps to synthesise simulated climate change across models. The Paleoclimate Model Intercomparison Project, now in its fourth phase (PMIP4; Kageyama et al., 2018) is a project endorsed by the Coupled Model Intercomparison Project phase 6 (CMIP6; Eyring et al., 2016), which aims to analyse and understand the differences between model simulations of past climates. PMIP4 has been updated from its earlier phase PMIP3 (Braconnot et al., 2012) by including additional past warm periods (Fig. 1), updated experimental designs and involvement of the new generation of climate models (Kageyama et al., 2018; Eyring et al., 2016).

The mid-Holocene (6000 years ago) and the Last Interglacial (127000 years ago) are characterised by altered seasonal and latitudinal distribution of incoming solar radiation when the Earth's orbits were different from modern. The *midHolocene* and *lig127k* experiments are Tier 1 PMIP4-CMIP6 simulations (Fig. 1)~~;~~ designed to examine the model response to changes in the Earth's orbit in periods when the atmospheric greenhouse gas concentrations were similar to the preindustrial level and the topographies and ice sheet size were also similar to modern. Otto-Bliesner et al. (2017) described the protocols and specific
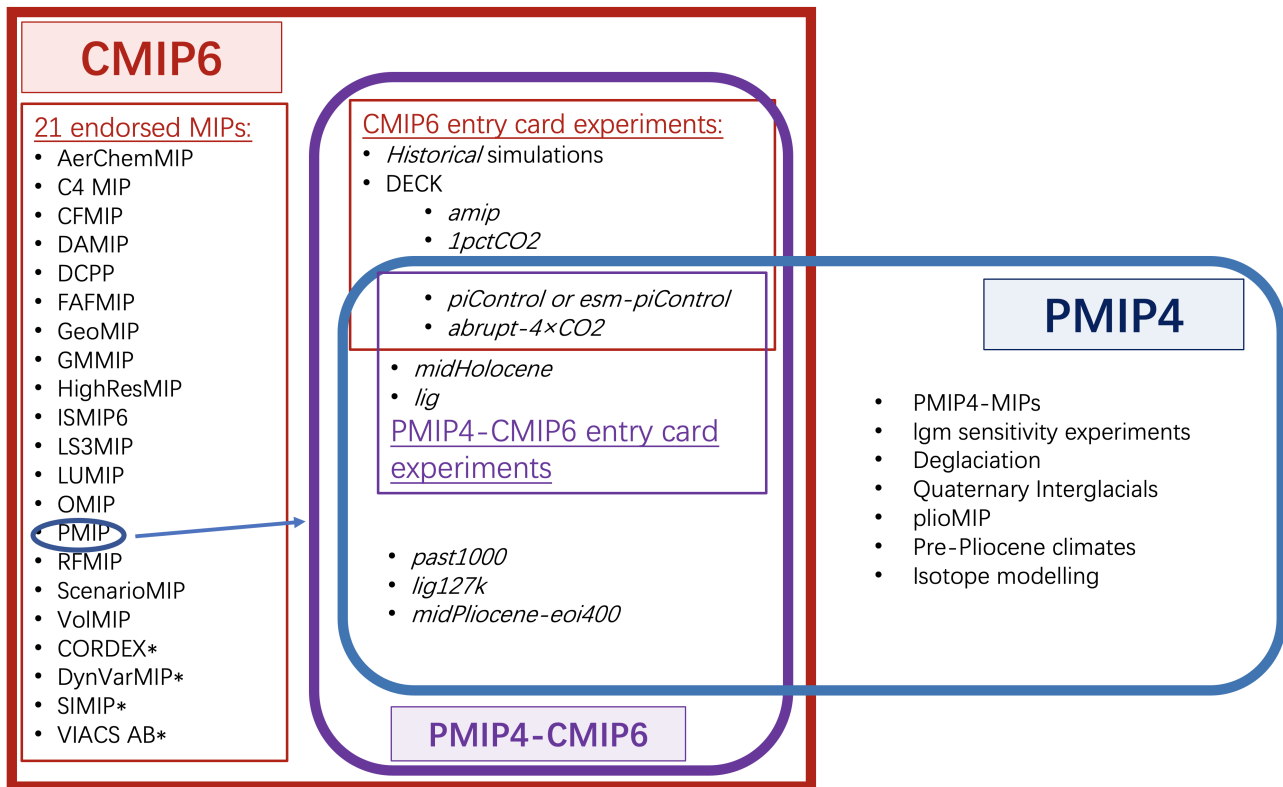
Figure 1. Schematic diagram illustrating the ~~PMIP4-CMIP6 experiments and their relationship to CMIP6 and PMIP4, according to Eyring et al. (2016) and Kageyama et al. (2018)~~CMIP6 and PMIP4 experiments after Eyring et al. (2016) and Kageyama et al. (2018). 'CMIP6' refers to the phase of the Coupled Model Intercomparison Project devised to support the IPCC's Assessment Report 6. 'PMIP4' is the fourth phase of Palaeoclimate Model Intercomparison Project. We refer to the subset of models and experiments in PMIP4 that are also part of CMIP6 (purple) as 'PMIP4-CMIP6'.

information for the two experiments in detail. Brierley et al. (2020) summarised the large-scale features in the PMIP4-CMIP6 *midHolocene* simulations and the changes since the previous generation (PMIP3-~~P~~CMIP5). Features in the PMIP4-CMIP6 *lig127k* ensemble have been analysed by Otto-Bliesner et al. (2021). These two ensembles within PMIP4 have contributed to the text in several chapters (Gulev et al., 2021; Eyring et al., 2021; Douville et al., 2021; Fox-Kemper et al., 2021) in the latest Sixth Assessment Report (AR6) of the Intergovernmental Panel on Climate Change (IPCC), as well as to figures in that report (Eyring et al., 2021).

PMIP4-CMIP6 model outputs have been standardised and uploaded on the Earth System Grid Federation (ESGF) servicing the diverse needs of various scientific communities (see Sect. 2 for more details). However, downloading these standardised files can be time consuming due to abundant variables and their available various temporal resolution etc. This means that

35 the files cannot be automatically downloaded via a single script. Processing the files to conduct ensemble analysis can also be complicated, because the simulations have differing time length and they use different spatial resolution specific to model configuration. Some methodological decisions are required through analysis. Therefore, a clear workflow and its saved outputs would be useful to reduce the effort to download and process the PMIP4-CMIP6 outputs.

Here we provide a detailed description of the workflow (Fig. 2) and scripts that have been used to create figures in the
40 primary description papers of the latest PMIP4-CMIP6 *midHolocene* (Brierley et al., 2020) and *lig127k* (Otto-Bliesner et al., 2021) experiments. The scripts have also been used for figures in multi-experiment papers coordinated by the past2future working group of PMIP on the PMIP3-CMIP5 tropical Atlantic inter-annual variability (Brierley and Wainer, 2018), PMIP3-CMIP5/6 climate variability (Rehfeld et al., 2020) and PMIP3-CMIP5 and PMIP4-CMIP6 ENSO (Brown et al., 2020) and contributed to Figures 3.2b and 3.11 in IPCC AR6 WG1 Chapter 3 (Eyring et al., 2021). In section 2, we give a description of
45 the PMIP4 output availability and a discussion of how to access data, along with an evaluation of how and when to apply the PaleoCalAdjust software. The following section (Sect. 3) describes the Climate Variability Diagnostics Package (CVDP) and how it has been modified for PMIP4 purposes. The general NCL and Python routines (as pmip_p2fvar_analyzer v1.0) used in the above papers are described in detail in section 4. Some case studies of possible analyses using the described workflow are given in section 5, followed by a short summary in section 6.

2 Collecting PMIP4 output
50

Each model participating in the CMIP6 has uploaded (or is going to) upload their DECK and historical simulations (and endorsed MIPs simulations if available) onto the Earth System Grid Federation (ESGF; Balaji et al., 2018, available at https://esgf-node.llnl.gov/search/cmip6/) in the standard format as required by the CMIP6 Data Request (Juckes et al., 2020). All CMIP6 outputs have been written to netCDF files with one variable stored per file ~~(9112 variables had been uploaded to PMIP4 by Dec~~
55 ~~2021)~~. The number of variables and simulations contributed by each model is available at the ESGF CMIP6 PMIP data holdings webpage (https://pcmdi.llnl.gov/CMIP6/ArchiveStatistics/esgf_data_holdings/PMIP/index.html) Full lists of variables in the ESGF controlled vocabulary are available at http://proj.badc.rl.ac.uk/svn/exarch/CMIP6dreq/tags/latest/dreqPy/docs/CMIP6_MIP_tables.xlsx. Users can restrict searching results by selecting appropriate search constraints (e.g. Variable, Experiment ID and Frequency). Table 1 lists the variables and their relevant information that we downloaded from the ESGF and used for
60 analysis. For each PMIP model on the ESGF, data was acquired for every single experiment in the DECK and PMIP4 (see Fig. 1). Only a single variant was selected for each experiment. The variant ID of CMIP metadata is defined in a format of 'r1i1p1f1', where r is realisation, i is initialisation, p is physics, f is forcing and each number is the index for the corresponding configuration. Only the FGOALS-g3 *midHolocene* has multiple runs, and r1i1p1f1 has been selected. There are 4 different forcings available for the IPSL-CM6A-LR (Braconnot et al., 2019) : only the r1i1p1f1 variant has been selected as that relates
65 to the Tier 1 *midHolocene* protocol.

A local replica of the PMIP data stored on the ESGF was created to facilitate the deployment of the tools described later. The curation approach was chosen that permitted the inclusion of simulations prior to their publication on ESGF, and allowed for

3

Table 1. List of variables in the *piControl, midHolocene* and *lig127k* simulations that were downloaded from the ESGF.

Long name	Variable name	Unit	Table ID
Near-Surface Air Temperature	tas	K	Amon
Surface Temperature	ts	K	Amon
Sea Level Pressure	psl	Pa	Amon
Precipitation	pr	kg m-2 s-1	Amon
Ocean Y Overturning Mass Streamfunction	msftyz	kg s^{-1}	Omon
Sea-Ice Area Percentage (Ocean Grid)	siconc	%	SImon

Information follows
http://proj.badc.rl.ac.uk/svn/exarch/CMIP6dreq/tags/latest/dreqPy/docs/CMIP6_MIP_tables.xlsx

a coherent treatment calendar-adjusted files. Since each experiment contained a single ensemble member, a revised database structure was adopted to harmonise both CMIP6 and CMIP5 ~~ensemble~~ collection conventions. The resulting database only has

70 two directory levels: the top level is taken as the model, with a sub-directory for each experiment that contains all the outputs listed in Tab. 1. Additionally an 'areacello'(i.e. grid-cell area for ocean variables) fixed variable is stored in each sub-directory for the computation of sea ice area on rotated grids. This was not always deposited on the ESGF for an experiment and needed to be sourced from elsewhere. This curation approach has the added advantage of permitting manual treatment of individual issues. Symbolic links were used to populate this curated ESGF replica where possible (to avoid the duplication of data files).

75 When many little files were stored on the ESGF, these were concatenated in a single larger file ~~in this instance~~ using the NetCDF Operators (Zender, 2008) to avoid I/O bottlenecks. Only years for which all output variables are available were used. This curation approach had the additional advantage permitting the inclusion of simulations prior to publication on ESGF, and allowed for a coherent treatment calendar-adjusted files. The file names of the resulting curated directory can be seen at https://github.com/pmip4/UCL_curated_ESGF_replica.

80 The eccentricity, obliquity and precession at the mid-Holocene and the Last Interglacial were different from those at 1850 CE. Therefore aggregating daily output to monthly averages using a 'fixed-length' calendar to define the number of days in each month is not appropriate across all the experiments: a 'fixed-angular' calendar should be used instead. Bartlein and Shafer (2019) provide software, `PaleoCalAdjust`, to convert between the two calendars for simulation output that are produced and stored in the general CMIP format. The approach taken by the PaleoCalAdjust software is to interpolate from non-adjusted

85 monthly averages down to pseudo-daily values, and then to aggregate those values back up to 'monthly' resolution for each 30° segments of Earth's orbit (see `adjusted_month_lengths.xlsx` on Github for adjusted month lengths). Bartlein and Shafer (2019) evaluated the software's performance for monthly temperature and precipitation variations and showed that in some situations the aliases due to the calendar definition can be larger than the climate change signal. Therefore, Brierley et al. (2020) and Otto-Bliesner et al. (2021) decided to apply the calendar adjustment when analysing seasonal temperature and

90　precipitation. Calculation of regional mean temperature of the warmest month (MTWA) and of the coldest month (MTCO) for the mid-Holocene in Fig 3.44 in IPCC AR6 WG1 (Eyring et al., 2021) used adjusted monthly temperatures.
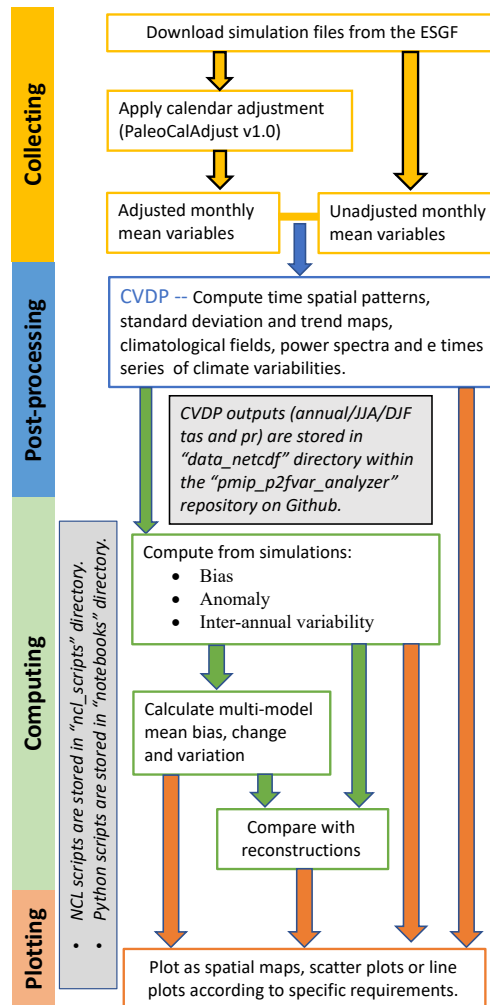

Figure 2. Schematic flowchart illustrating the processes within this workflow.

Brierley et al. (2020) explored the potential interpolation errors from PaleoCalAdjust on precipitation in monsoon regions (Pollard and Reusch, 2002) by analysing the averaged rain rate during the monsoon season over the South American monsoon domain in the IPSL-CM6A-LR *midHolocene* experiment. As a result, Brierley et al. (2020) decided to not apply the calendar adjustment when analysing monsoon variables while presenting DJF and JJA precipitation changes that did use it. In general, whether it is better to use PaleoCalAdjust depends on the steps in the subsequent processing and analysis. If scripts average many months without weighting by month length then we feel it is undesirable to use PaleoCalAdjust (although future versions of the software may additionally conserve the annual means). The monthly palaeoclimate plots in the IPCC Interactive Atlas (Guiterrez et al., 2021; Gutiérrez et al., 2021), available at https://interactive-atlas.ipcc.ch/, are calendar adjusted, whilst the annual mean fields are computed as a unweighted average of the 12 un-adjusted monthly climatology (Brierley and Zhao, 2021a). This means that users will not be able recreate the annual mean themselves by downloading and averaging the 12 monthly fields, unless they weight them by the number of days in the month. Gutiérrez et al. (2021) also provide equivalent climatologies for the *midPliocene-eoi400*, *lgm* and *lig127k* ensembles.These were created using the workflow described here (Brierley and Zhao, 2021a). Both the Interactive Atlas (Gutiérrez et al., 2021) and the data accompanying this manuscript contain only the subset of models which had uploaded output onto the ESGF. This difference is most marked for the *midPliocene-eoi400* and *lgm*, where images within the IPCC report (Gulev et al., 2021; Eyring et al., 2021) use the larger ensemble of Haywood et al. (2020) and Kageyama et al. (2021) that included non-CMIP6 models.

3 Post-processing of PMIP4 output

The Climate Variability Diagnostics Package (CVDP; Phillips et al., 2014) was developed by the National Center for Atmospheric Research (NCAR)'s Climate Analysis Section to improve and facilitate the evaluation of major modes of internannual climate variability, like El Niño-Southern Oscillation (ENSO) and Atlantic Multi-decadal Oscillation (AMO), in models and observations. This package computes spatial patterns, standard deviation and trend maps, climatological fields, power spectra and time series of climate variables any user-specified set whose files fit CMIP5/CMIP6 output requirements. Analysis results of each model are presented via webpages, which also include a summary table comparing model performance against any chosen observations. For later use, output is saved in a netCDF file that contains the data fields that are plotted in each .png image. This package has been used by Fasullo et al. (2020) to evaluate the representation of climate variability in the CMIP6. The CVDP source code, as well as output files for historical and future scenario simulations, can be downloaded from http://www2.cesm.ucar.edu/working-groups/cvcwg/cvdp.

The CVDP has been adapted for palaeoclimate purposes. Brierley and Wainer (2018) introduced additional coupled modes of variability in the Tropical Atlantic. Brown et al. (2020) altered the compositing of ENSO events to other seasons not just DJF. Additionally, they computed La Niña and El Niño composites separately, although these were not used in the publication. Otto-Bliesner et al. (2021) introduced the computation of time series of sea ice area, in addition to sea ice extent.

Brierley et al. (2020) introduced the calculation of a global monsoon domain by applying two criteria (a) annual range (local summer - local winter) of precipitation rate is greater than 2 mm d^{-1} and (b) the local summer rainfall exceeds 55% of the

125 annual total (Wang and Ding, 2008; Wang et al., 2011, 2014). Notably, our criteria differs from the definitions used in the IPCC AR6 WG1 in which the global monsoon is defined as the region where the annual range of precipitation exceeds 2.5 mm d^{-1} as in Kitoh et al. (2013); IPCC (2021). The domain~~'s~~for extent is calculated separately for each individual monsoon season ~~in~~for each year and its extent and area-averaged rain rate computed. This differs slightly from analyses of future projections, where domains are fixed at their present-day extent (Christensen et al., 2013; Douville et al., 2021). For regional monsoons, we follow

130 the delineation ~~of regional monsoons~~ adopted for IPCC AR5 (Christensen et al., 2013), because those adopted for AR6 (IPCC, 2021) have poleward extents that are not appropriate under altered orbital configurations. The monsoon diagnostics were also analysed by Otto-Bliesner et al. (2021).

There are also some further modifications to the PMIP version of the CVDP package that have not been previously documented.

– The mean and standard deviation spatial fields are only computed over the years used to compute the climatology. This
135 makes no difference unless a `custom_climo` is set (the default is to use all available years). It allows the climate state at a particular point in a transient simulation to be isolated, and is generally only used to select the end of the *abrupt4xco2* and *1pctco2* experiments, or to select the satellite period in the *historical* experiment.

– The temperatures of the warmest month and the coldest month are computed, along with their (interannual) standard deviations. Pollen data are often used to reconstruct these variables, so calculating comparable fields from the climate
140 models can be helpful. As a comparison between the Bartlein et al. (2011) reconstructions and *midHolocene* simulations only features in the supplemental of Brierley et al. (2020), the inclusion of these variables was not documented in the manuscript~~'s~~ methodology.

– The principal-component based definition of the AMOC advocated by Danabasoglu et al. (2012) has been abandoned. We revert to a more-conventional definition: taking the AMOC as the maximum zonal mean streamfunction at 30°N below
145 500m. This was motivated by the conflation of mean state changes and variability arising from the linear detrending in the principal-component based definition, which is not appropriate for simulations running from 850 CE to present (Otto-Bliesner et al., 2016).

– Time series of area-average precipitation and surface air temperature are calculated for 58 regions. These consist of 30° latitude bands (over land and sea) as well as the climate regions presented in the IPCC report (AR5 regions; Collins
150 et al., 2013). These time series are stored as variables named `ipcc_TLA_pr` and `ipcc_TLA_tas` respectively, where TLA is the conventional three letter acronym for the AR5 regions and a text string for the latitude bands. It is worth mentioning that currently the use of the present-day land-sea mask is hardwired into the CVDP.

– Monthly time series plots of the new monsoon and area-average diagnostics are written so that only a low resolution mean and spread are visualised for records greater than 150 years. This is more computationally efficient than calculating and
155 presenting high resolution data.

– The webpages created when running the CVDP have been altered to accommodate the new diagnostics. These are collated together to frorm a resource ~~we have previously~~ called the 'PMIP Variability Database' ~~(Brierley and Wainer, 2018)~~ by Brierley and Wainer (2018). It is accessible from http://past2future.org/.

4   Plotting post-processed outputs

160   A series of scripts have been developed that use the CVDP summary output files as inputs for ensemble analysis. Initial development of these scripts was in NCL by Brierley and Wainer (2018) to complement the original package. Similar to the CVDP , they consist of a library of common functions and individual NCL scripts that convert these functions into (sets of) figures. In the build up to CMIP6, the decision was made to pivot this component of the workflow into Python. This allows for greater interactivity by users through notebooks and JupyterHubs, as well as better explanation of any example cases. The

165   repository containing these Python scripts is called the pmip_p2fvar_analyzer v1 (see the "Code and data availability" section). We recommend that users adopt the pPython scripts unless they are already expert in NCL. The documentation available for python is more extensive, both within these scripts and across the wider climate science community.

4.1   NCL

All the NCL scripts require a series of functions from `cvdp_data.functions.ncl`. These functions (Tab. 2) are them-

170   selves divided into three classes: those that return graphics, those that return statistics or tables, and those that are related to the identification and loading of simulation files. These functions are intended to operate on a directory containing the CVDP summary files and output figures(s) or table(s) directly. All regridding and ~~ensemble~~ multi-model averaging is performed on the fly, although alternate functions have been written to output the data as netcdf files. NCL avoids the need to specify many keywords in function calls by attaching them as 'attributes' to a single logical variables (in a similar fashion that metadata

175   is attached to a netCDF variable). The plotting routines we have written allow 'resources' to be passed to them in the standard NCL fashion, providing a high-level of control over the resulting images. These routines can also accept supra-resources, which are logical flags turning on additional functions, for example CONSISTENCY=True will additionally overlay hatching to indicate when the ensemble is consistent in its signal (as seen in Rehfeld et al., 2020). The NCL routines were used to make all the figures in Brierley and Wainer (2018) and Brown et al. (2020), as well as contributing the first 3 figures of Rehfeld et al.

180   (2020).

4.2   Python

Similar to the NCL scripts, most of the analysing and plotting processes in Python have been written into functions, but they are stored in different scripts according to their purposes instead of being written in a single script. Each script was written in notebook format (see Sect. 4.3 for reasons) and named according to its purpose and usage with detailed documentation available

185   in the script. The scripts are built upon the powerful `xarray` package (Hoyer and Hamman, 2017). These scripts all start with a set of five functions to collect the names of available models that have the variable in the experiment and their corresponding

Table 2. The NCL functions and procedures created to support analyses of the CVDP summary files. They are categorised according to whether they return a graphic, a statistic, or produce no output at all to the user and are intended to be called internally. **Bold** font indicates a procedure, the rest are functions.

graphics	statistics	internal
plotCVDPcomparisonMaps	extract_latlon_areastat	find_files_wVar
plotDiffEnsMnMaps	stat_ts_var	read_latlon_var
plotEnsTimeseries	**createTableGCMsExptsYears**†	read_diff_latlon_var
plot_output_CVDPmap*		find_pair_files_wVar
plot_output_DiffEnsMn*		read_ts
		read_ts_all
		createGCMsNameDictionary
		translateGCMsNameDictionary

*returns a netCDF file, as well as an graphic. †returns a LaTeX formatted table.

directory and filenames respectively and return a dictionary storing these information as "'model_name':'directory/filename'" (hereafter referred as "target-filename dictionary"), ~~in which f~~. Function identify_ensemble_members requires running find_experiment_ensemble_members.bash in bin directory to identify available ensemble members (i.e. model names) whose simulations have the target variable in the experiment. Same as the NCL scripts, all regridding and ~~ensemble~~ multi-model averaging in Python scripts is performed on the fly, and the output can be saved as either a netCDF file or a csv file based on its type, if the user requires. We also have developed a set of plotting schemes in which colours are chosen according to the colour guidelines provided by IPCC-WG1 (available at https://github.com/IPCC-WG1/colormaps; last assessed on 17th May 2021). Some examples of possible usage are given in section 5.

4.3 Interactive Application

One advantage of the Python scripts over the NCL equivalent is their wider user base. Python notebooks allow documentation and outputs to be stored with the scripts. A logical next step is to permit users to interact with the scripts. Attempts using Binder (https://mybinder.org/) to create a cloud-computing deployment were found to be underpowered - in part because of the two different coding languages and any data that should be stored along with them. Our solution to this problem is to instead use Docker (https://www.docker.com/) to create a containerised application. In this context, the Docker image appears to be a virtual machine ~~that~~ stor~~es~~ing both required software packages and data, as well as providing a quick and easy method of developing scripts by external users.

Docker images are a hybrid mix of the Linux kernel and bespoke local runtime environment. The Docker image is used to configure and distribute the state of an application. The state of the application in the current context refers to libraries and stored data sets. Dissemination of Docker images via well-known web-services such as DockerHub. The combination of par-

ticular software versions (and dependencies) as well as data has been recognised as a useful venue for research reproducibility (Boettiger and Eddelbuettel, 2017; Nüst et al., 2020).

In a host computer equipped with the Docker run-time (widely available for most common operating systems), the Docker image recreates the original system, and the user can access the image either via the command line, or as intended here, using the Jupyter framework via a web browser installed on the host computer. Given that the Docker image may be running on an underpowered computer (e.g., a standard laptop), there are computational limits to what is practical to achieve with this setting. The inclusion of post-processed summary data in the image will however allow users to run analysis in typical laptops. The Docker image is available at https://github.com/pmip4/pmip_p2fvar_analyzer - instructions explaining how to use it are included in the documentation at https://pmip-p2fvar-analyzer.readthedocs.io/. In practice, this requires the user downloading and installing the Docker run time for their operating system, and pointing the Docker run time to the image on the Internet.

The repository, and therefore the interactive image, contains a series of summary data of the whole ensemble, as well as a script to download the CVDP output for each individual simulation. The summary data are a series of comma-separated value tables (`data_frames` in Python terminology), which collect together single pieces of information across each simulation. For example, the file `ESGF_doi.csv` contains the digital object identifier for each simulation – an important piece of information that should be included in PMIP4 publications to both improve traceability and provide due credit to those having performed the runs. We provide the long-term mean and standard deviation of the interannual time series of area-averaged temperature and precipitation for each region identified by (Collins et al., 2013), in the AR5_Regions sub-directory. Statistics of the newly created regional monsoon domains (described in Sect. 3, and plotted in Fig. 7) are included in the `monsoon_domains` sub-directory. Some ~~oft-computed~~ metrics that are often computed are tabulated in the `common_measures` sub-directory – the long-term~~,~~ global mean surface temperature table also includes each model's CMIP generation and equilibrium climate sensitivity (ECS; from Andrews et al., 2012; Zelinka et al., 2020). The temperature changes averaged for 30° latitude bands over the land and ocean are included in the `tempchange_latbands` sub-directory, along with similar tables taken from the supplementary information of PMIP publications. These files form the basis of Fig 3.2b in IPCC AR6 WG1 (Eyring et al., 2021), and provide the global mean surface temperature in palaeo periods as estimated from climate models as reported in the Technical Summary (Arias et al., 2021) and Chapter 2 (Gulev et al., 2021). The CVDP computes many different modes of variability for each simulation (Sect. 3), and the amplitudes of these are tabulated in the `climate_modes` sub-directory. For indices based on area-averaged SST, these are simply the standard deviation of the time series. For modes identified using principal component analysis, the approach of Rehfeld et al. (2020) is adopted and the amplitude is the spatial standard deviation of EOF pattern averaged over same region as the analysis.

5 Example~~s~~ ~~U~~uses

By choosing and applying appropriate functions in the scripts, the workflow can produce analyses of temperature, precipitation and monsoon characteristics (and other climatic patterns if required). These analyses can involve just the ~~ensemble~~ multi-model mean or individual models and return the outputs as figures (spatial maps or scatter plots etc) or data files (as netCDF or csv) as
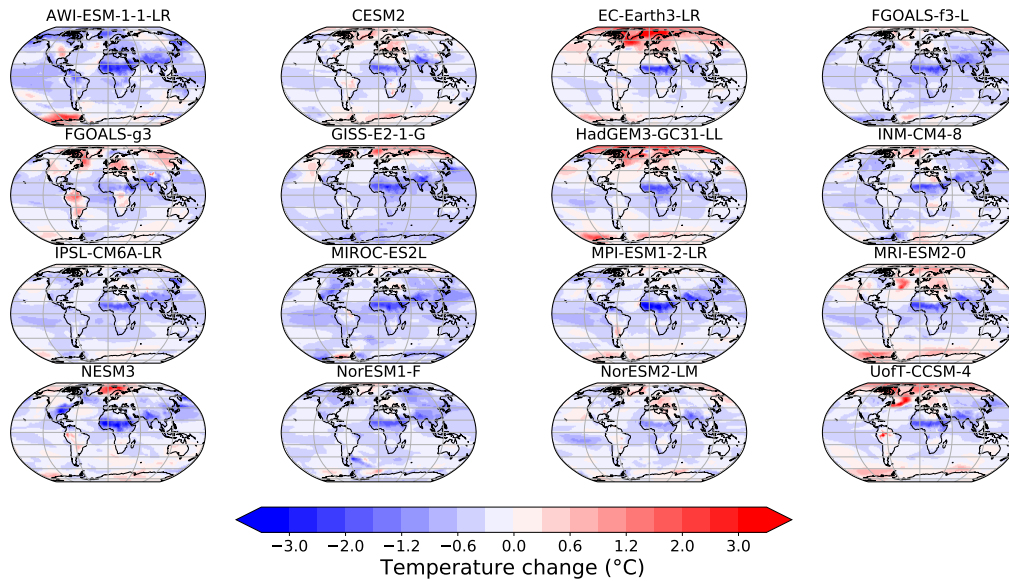
Figure 3. Annual mean surface temperature change (°C) in the *midHolocene* as simulated by individual models that features Fig. 4 and Fig.1a in Brierley et al. (2020). Anomalies have been regridded to 1° by 1° resolution.

required. Detailed documentation of the scripts and functions are available elsewhere (such as in the accompanying notebooks), so will not be repeated here. Instead we provide some worked examples of output to help readers get an idea of the possible options. These examples have generally already been featured in PMIP publications or are alluded to in them.

5.1 Plotting spatial patterns

The first example (Fig.3) is the annual mean temperature difference between the *midHolocene* ~~minus~~and the ~~piControl~~*piControl*, which shows the patterns of temperature change produced by each model in the PMIP4-CMIP6 *midHolocene* ensemble that features in Brierley et al. (2020). Fig. 3 is generated by using the function `Calculation_ensemble_change('PMIP4',` `'midHolocene','tas_spatialmean_ann','model')` to return a directory containing the regridded annual mean temperature change produced by each model (referred as tas_data) and the function `plot_ensemble_tas(tas_data,'ann')` to plot those temperature changes.

The process used to create Fig.3 has four major steps:

1. generate target-filename dictionaries for the *midHolocene* and the *piControl* that have the specified variable;

2. search to see which models occur in both directories, as well as the prescribed list of PMIP4 model names;

11
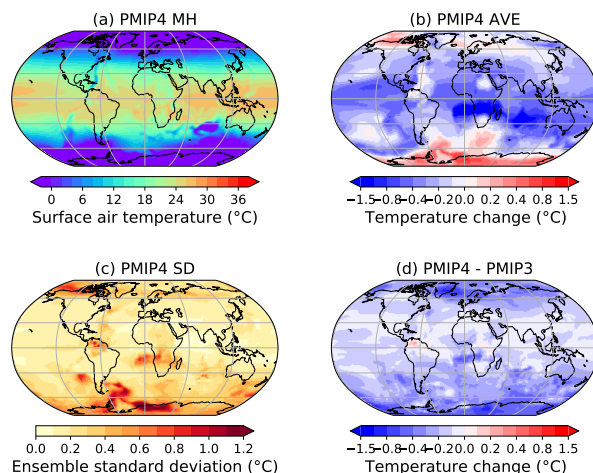
Figure 4. Annual mean surface temperature in the *midHolocene* simulations (°C). (a) The ~~ensemble~~ multi-model mean, mid-Holocene annual mean surface temperature simulated by PMIP4-CMIP6 *midHolocene* simulations. (b) The ~~ensemble~~ multi-model mean, annual mean temeperature changes in PMIP4- CMIP6 (*midHolocene – piControl*) and (c) the inter-model spread, defined as the across-ensemble standard deviation. (d) The difference in the ~~ensemble~~ multi-model mean, annual meamn temperature changes between the PMIP4-CMIP6 and the PMIP3-CMIP5. Panels (a), (b) and (c) are replotted from panels a, b and e in Fig.1 of Brierley et al. (2020) respectively.

3. loop through the matching model's *midHolocene* and *piControl* simulations individually and then compute the difference (i.e. *midHolocene - piControl*);

4. regrid the difference to 1° by 1° resolution (in order to easily calculating the ~~ensemble~~ multi-model mean) and then
255   stored in the output dictionary named as the model name.

The same function can be used to produce ~~ensemble~~ multi-model mean analysis, e.g. the ~~ensemble~~ multi-model mean of annual mean surface temperature in the PMIP4-CMIP6 *midHolocene* ensemble shown in Fig. 4, by entering `'mean'` instead of `'model'` used in example 1. This choice requires an additional step: calculate and return the multi-model average and the standard deviation across the ensemble. The NCL programmes do not have the ability to set a flag to determine whether to
260   compute the ~~ensemble~~ multi-model mean or individual panels for each ensemble member. Instead they determine the ensemble behaviour depending on the dimension of files containing the requested input variables. If a difference plot (called using `plotDiffEnsMnMaps`) detects multiple files for each input, then it will compute a~~n~~ ~~ensemble~~ multi-model average of the anomalies. Should the second named experiment resolve to only a single file, then the anomaly between each ensemble member and this file will be computed (this functionality was built to compute the ~~ensemble~~ multi-model mean of the biases
265   from a single observational dataset). We provide example code (`multi-panel_plot.ncl`) that was used to create Fig.

12

7 of Brown et al. (2020). This script also demonstrates two of the supraresources: CONSISTENCY=True provides stippling to highlight where at least two-thirds of the ensemble members show the same sign of anomaly as the ~~ensemble~~ multi-model mean; whilst OVERLAY_CONTROL=True adds contour lines showing the ~~ensemble~~ multi-model mean of the variable in the second experiment named (~~"~~"piControl" in this case.).

5.2 Plotting oceanic patterns – the Atlantic Meridional Overturning Circulation (AMOC)

The output files from the CVDP can be used as input for computing ~~ensemble~~multi-mean AMOC changes (~~mid-Holocene - piControl~~ *midHolocene - piControl*) in PMIP4 simulations. The variable called 'amoc_mean_ann', which is analysed with the modified version of the CVDP for individual model~~s~~ simulations, is loaded by Iris for both the mid-Holocene and ~~piControl~~ *piControl* ~~experiment~~ensembles, then all ~~models~~ CVDP outputs are regridded on to a 1° latitude grid with 61 depth levels between 0-6000m. This process is achieved through Iris cube's interpolation and regridding schemes called `iris.analysis.Linear()`. Since models can have different names for their dimension coordinates, basic cube mathematics can not be done directly. Therefore, only the regridded data in each model are extracted for calculating the differences and averages at this stage. The ~~ensemble~~ multi-model mean AMOC change is computed by taking ~~the average of the regridded changes produced by individual models~~ the same steps as in Section 5.1. After that, the model-averaged data are put back into one of the regridded models in order to use its dimension coordinates for further plotting. The figure is plotted using 'iris.quickplot' which provides a visualisation for a cube with a title, x and y labels and a colorbar where appropriate.

In addition, the 'amoc_mean_ann' variable derived from the CVDP output files can also be used as an input for generating the AMOC profile for a specific latitude, e.g. 30^oN. This is helpful when comparing the AMOC strength throughout all depths in different PMIP4 experiments, and was used to create the scatter plot of AMOC values shown in Fig. 10 of Brierley et al. (2020).

5.3 Plotting time series

The CVDP can also be used to analyse and generate time series data. Fig 6 gives an example of the analysed results of calendar adjusted monthly mean sea ice areas (defined as sea ice fraction multiplied by the area of each grid cell) in the Arctic in the *midHolocene* and *piControl* simulations. Lines are coloured following the standard CMIP6 model colour scheme (available at https://github.com/IPCC-WG1/colormaps/blob/master/CMIP6_color.xlsx~~; last assessed on 30th Nov 2021~~).

5.4 Computing statistics

Our scripts can compute statistics from the output files created by the CVDP. The simplest statistics that might be needed is the length of the data records for a particular variable. The example script `generate_model_table.ncl` interrogates the directory to extract the number of years available for every simulation containing a variable called `nino34` performed under series of specified experiments. The resulting table can either be output as a spreadsheet (as comma separated values) or in a format to be directly inputted into a LATEX manuscript.

**13**
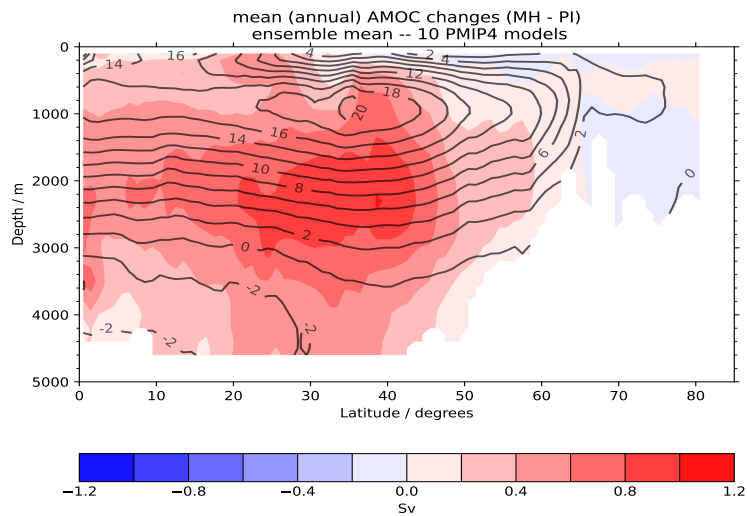
Figure 5. ~~Ensemble~~ Multi-model mean plots for AMOC spatial structure changes between the ~~midHolocene~~*midHolocene* and ~~piControl~~*piControl*. 11 PMIP4 models which performed midHolocene experiment are used for plotting the ~~ensemble~~ multi-model means. The overlaid contours (black lines show AMOC strength in the ~~piControl~~*piControl* for locating the maximum AMOC.

Given a monthly mean precipitation netCDF file as an input, the CVDP outputs time series of monsoon rainfall rate (Fig. 7a) and areal extent (Fig. 7b) of each regional monsoon (Sect. 3). Fig. 7 is the result of this computation for the North African Monsoon. It uses these time series to compute relative changes in monsoon characteristics in the *midHolocene* experiment relative to the *piControl* and shows the five available diagnostics (Brierley et al., 2020).

It is also possible to compute areal statistics from the latitude-longitude fields. As part of our modifications to the CVDP, area-weighted average monthly time series for the AR5 regions are now computed for both precipitation and temperature (Sect. 3). To cope with the modification of those regions for AR6 (Iturbide et al., 2020), the area-average precipitation changes shown in Fig.3.11 of Eyring et al. (2021) are instead computed from the 2D "pr_spatialmean_ann" variable. An alternate approach to look at the poleward extension of the areal extent of the North African monsoon is to compute the most northerly latitude ~~to which the monsoon~~ reache~~s~~d by the monsoon (as in Tab. S2 of Brierley et al., 2020). Fig. 8 gives an example of the NAF expansion in the *midHolocene* and *lig127k* ensembles. We define a series of functions to determine the change in latitude where the zonal mean summer (MJJAS) rain rate (stored in the files as "monsoon_summer_rainrate") equals 2 mm d^{-1} over the North Africa (15°W–30°E). See the corresponding notebook for details.
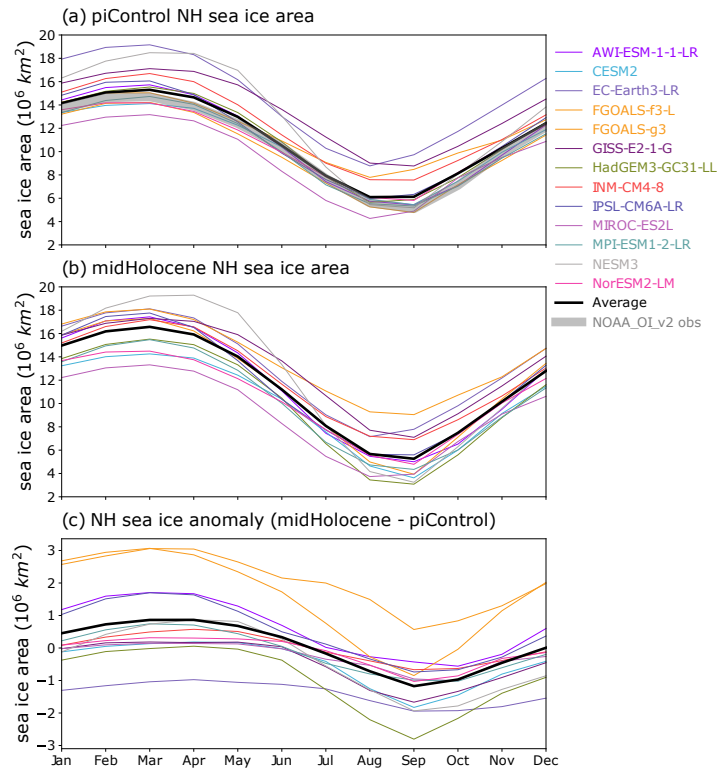
Figure 6. Annual cycle of the Arctic sea ice area ($10^6\ km^2$) for the (2) *piControl*, (b) *midHolocene* and (C) their anomaly (*midHolocene - piControl*), replotted from Fig.17 of Otto-Bliesner et al. (2021). The grey line in panel (a) shows the observed monthly mean sea ice areas from the NOAA_OI_v2 dataset for 1982 - 2001 (Reynolds et al., 2002).
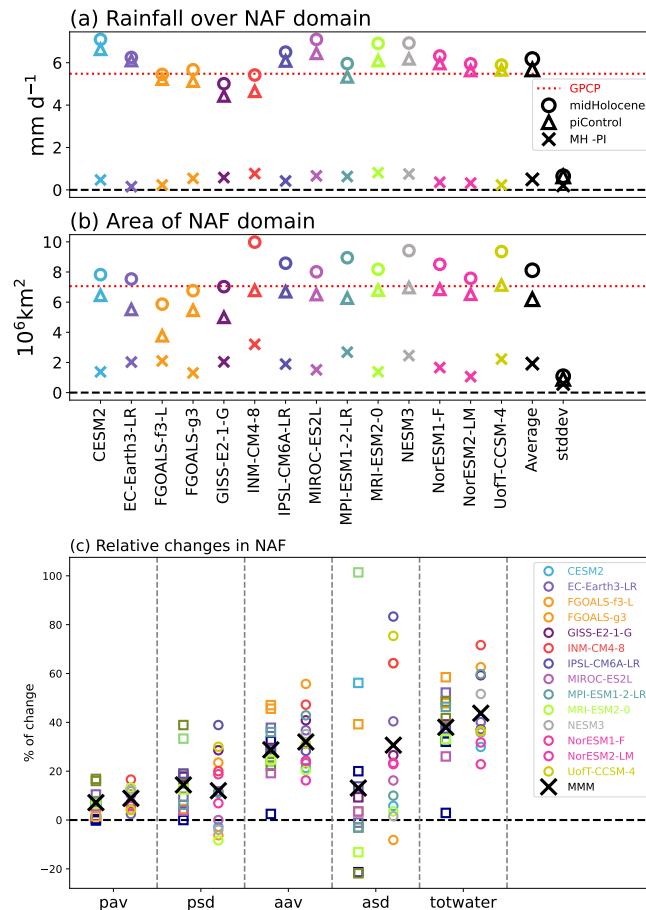
Figure 7. Changes in the the North African Monsoon (NAF) (a) Area-averaged NAF monsoon summer rain rate (mm d^{-1}) in the *midHolocene* (circles) and *piControl* (triangles) simulations and the difference between them (*midHolocene - piControl* in crosses). **(b) same as panel (a) but for the areal extent of NAF**. The red dotted lines in panels (a) and (b) show the corresponded climatology seen in the 1971-2000 GPCP observational dataset (Adler et al., 2003). **(c)** Relative changes (Brierley et al., 2020) five different monsoon diagnostics beginning from left in order are change in area-averaged monsoon summer rain rate (**pav**), change in the standard deviation of interannual variability in the area-averaged monsoon summer rain rate (**psd**), the change in the areal extent of the NAF monsoon domain (**aav**), change in the standard deviation of interannual variability in the areal extent of the NAF monsoon domain (**asd**) and the percentage change in the total amount of water precipitated in each monsoon season computed as the precipitation rate multiplied by the areal extent (**totwater**). Colours follow the standard colours for CMIP6 models used in the IPCC AR6. If a PMIP3-CMIP5 model (square) is an earlier version of a PMIP4-CMIP6 model, it is coloured same as the PMIP4-CMIP6 one, otherwise coloured by dark blue.
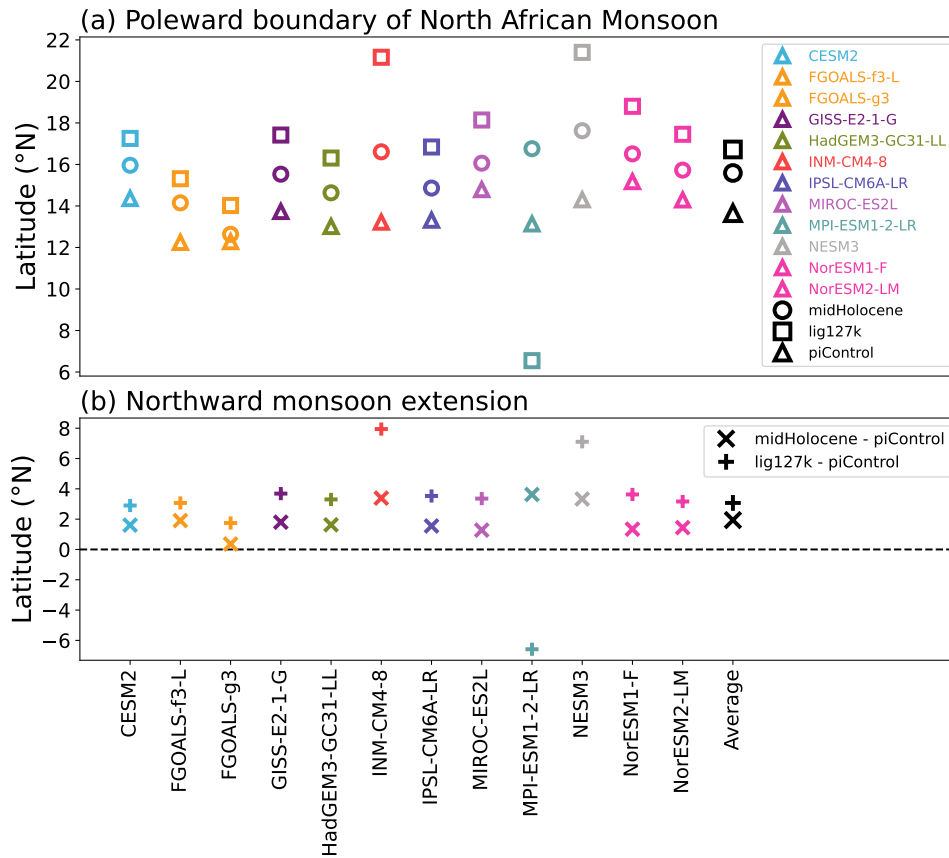
Figure 8. NAF monsoon poleward extension in the PMIP4-CMIP6 *midHolocene* and *lig127k* ensembles. (a) The latitude of the poleward boundary of the NAF monsoon in the simulations and (b) the northward monsoon extension. The ~~latitude of the~~ boundary is ~~calculated by determining the change in~~ the latitude where the zonal mean summer (MJJAS) rain rate equals to 2 mm d^{-1} over the North Africa (15°W–30°E)

6 Summary

The simulations that have been performed for PMIP4-CMIP6, and the large amount of model output available from them, are a great resources for understanding past climates. The procedure by which this model output is analysed as an ensemble can be time-consuming and involve some methodological decisions. Here we have described the way that our group have chosen to perform our recent analyses (Brierley et al., 2020; Otto-Bliesner et al., 2021; Brierley and Wainer, 2018; Rehfeld et al., 2020; Brown et al., 2020). We document the approach used to obtain and curate PMIP4-CMIP6 simulations, process those outputs via the Climate Variability Diagnostics Package (CVDP), and then continue through to compute ensemble-wide statistics and create ensemble figures. We know from personal experience that replicating the results from published work can often involve reverse engineering the decisions made by researchers during their data processing, and that th~~ise~~e work presented in this manuscript removes the need for such effort.

PMIP4 only exists because of the spirit of openness and cooperation within its community, which neatly combines with the IPCC's desire for greater transparency about the figures and data contained within Assessment Report 6. Through documenting our workflow here, we continue in that vein. Hopefully our efforts, such as collation of all the PMIP-related DOIs, make it easier for others to also be transparent in their research.

The main contribution of this work is not the documentation though - rather it is the provision of post-processed files for each PMIP4-CMIP6 simulation alongside scripts to readily convert them into publication ready figures and tables. The interactive application should increase further lower the barriers to analysis of palaeoclimate model research. We hope that readers are inspired with ideas of potential analyses that they themselves can perform quickly and easily by using the results of our workflow and scripts as tools to analyse PMIP4-CMIP6 simulations.

References

Adler, R. F., Huffman, G. J., Chang, A., Ferraro, R., Xie, P.-P., Janowiak, J., Rudolf, B., Schneider, U., Curtis, S., Bolvin, D., Gruber, A., Susskind, J., Arkin, P., and Nelkin, E.: The version-2 global precipitation climatology project (GPCP) monthly precipitation analysis (1979–present), Journal of hydrometeorology, 4, 1147–1167, https://doi.org/10.1175/1525-7541(2003)004<1147:TVGPCP>2.0.CO;2, 2003.

Andrews, T., Gregory, J. M., Webb, M. J., and Taylor, K. E.: Forcing, feedbacks and climate sensitivity in CMIP5 coupled atmosphere-ocean climate models, Geophysical Research Letters, 39, 2012.

Arias, P. A., Bellouin, N., Coppola, E., Jones, R. G., Krinner, G., Marotzke, J., Naik, V., Palmer, M. D., Plattner, G.-K., Rogelj, J., Rojas, M., Sillmann, J., Storelvmo, T., Thorne, P. W., Trewin, B., Achuta Rao, K., Adhikary, B., Allan, R. P., Armour, K., Bala, G., Barimalala, R., Berger, S., Canadell, J. G., Cassou, C., Cherchi, A., Collins, W., Collins, W. D., Connors, S. L., Corti, S., Cruz, F., Dentener, F. J., Dereczynski, C., Di Luca, A., Diongue Niang, A., Doblas-Reyes, F. J., Dosio, A., Douville, H., Engelbrecht, F., Eyring, V., Fischer, E., Forster, P., Fox-Kemper, B., Fuglestvedt, J. S., Fyfe, J. C., Gillett, N. P., Goldfarb, L., Gorodetskaya, I., Gutierrez, J. M., Hamdi, R., Hawkins, E., Hewitt, H. T., Hope, P., Islam, A. S., Jones, C., Kaufman, D. S., Kopp, R. E., Kosaka, Y., Kossin, J., Krakovska, S., Lee, J.-Y., Li, J., Mauritsen, T., Maycock, T. K., Meinshausen, M., Min, S.-K., Monteiro, P. M. S., Ngo-Duc, T., Otto, F., Pinto, I., Pirani, A., Raghavan, K., Ranasinghe, R., Ruane, A. C., Ruiz, L., Sallée, J.-B., Samset, B. H., Sathyendranath, S., Seneviratne, S. I., Sörensson, A. A., Szopa, S., Takayabu, I., Treguier, A.-M., van den Hurk, B., Vautard, R., von Schuckmann, K., Zaehle, S., Zhang, X., and Zickfeld, K.: Technical Summary, in: Climate Change 2021: The Physical Science Basis. Contribution of Working Group I to the Sixth Assessment Report of the Intergovernmental Panel on Climate Change, edited by Masson-Delmotte, V., Zhai, P., Pirani, A., Connors, S. L., Péan, C., Berger, S., Caud, N., Chen, Y., Goldfarb, L., Gomis, M. I., Huang, M., Leitzell, K., Lonnoy, E., Matthews, J., Maycock, T. K., Waterfield, T., Yelekçi, O., Yu, R., , and Zhou, B., Cambridge University Press, 2021.

Balaji, V., Taylor, K. E., Juckes, M., Lawrence, B. N., Durack, P. J., Lautenschlager, M., Blanton, C., Cinquini, L., Denvil, S., Elkington, M., Guglielmo, F., Guilyardi, E., Hassell, D., Kharin, S., Kindermann, S., Nikonov, S., Radhakrishnan, A., Stockhause, M., Weigel, T., and Williams, D.: Requirements for a global data infrastructure in support of CMIP6, Geoscientific Model Development, 11, 3659–3680, https://doi.org/10.5194/gmd-11-3659-2018, https://gmd.copernicus.org/articles/11/3659/2018/, 2018.

Bartlein, P. J. and Shafer, S. L.: Paleo calendar-effect adjustments in time-slice and transient climate-model simulations (PaleoCalAdjust v1.0): impact and strategies for data analysis, Geoscientific Model Development, 12, 3889–3913, https://doi.org/10.5194/gmd-12-3889-2019, 2019.

Bartlein, P. J., Harrison, S., Brewer, S., Connor, S., Davis, B., Gajewski, K., Guiot, J., Harrison-Prentice, T., Henderson, A., and Peyron, O.: Pollen-based continental climate reconstructions at 6 and 21 ka: a global synthesis, Climate Dynamics, 37, 775–802, https://doi.org/10.1007/s00382-010-0904-1, 2011.

Boettiger, C. and Eddelbuettel, D.: An Introduction to Rocker: Docker Containers for R, The R Journal, 9, 527–536, https://doi.org/10.32614/RJ-2017-065, https://doi.org/10.32614/RJ-2017-065, 2017.

Braconnot, P., Harrison, S. P., Kageyama, M., Bartlein, P. J., Masson-Delmotte, V., Abe-Ouchi, A., Otto-Bliesner, B., and Zhao, Y.: Evaluation of climate models using palaeoclimatic data, Nature Climate Change, 2, 417–424, https://doi.org/10.1038/nclimate1456, 2012.

Braconnot, P., Zhu, D., Marti, O., and Servonnat, J.: Strengths and challenges for transient Mid-to Late Holocene simulations with dynamical vegetation, Climate of the Past, 15, 997–1024, https://doi.org/10.5194/cp-15-997-2019, 2019.

390 Brierley, C. and Wainer, I.: Inter-annual variability in the tropical Atlantic from the Last Glacial Maximum into future climate projections simulated by CMIP5/PMIP3, Climate of the Past, 14, 1377–1390, https://doi.org/10.5194/cp-14-1377-2018, 2018.

Brierley, C. and Zhao, A.: PMIP_for_AR6_Interactive_Atlas, GitHub, https://github.com/chrisbrierley/PMIP_for_AR6_Interactive_Atlas, last access: 12 July 2021, 2021a.

Brierley, C. and Zhao, A.: pmip4/pmip_p2fvar_analyzer: Making new release to create DOI, Zenodo,
395 https://doi.org/10.5281/zenodo.5242948, last access: 24 Aug 2021, 2021b.

Brierley, C. M., Zhao, A., Harrison, S. P., Braconnot, P., Williams, C. J. R., Thornalley, D. J. R., Shi, X., Peterschmitt, J.-Y., Ohgaito, R., Kaufman, D. S., Kageyama, M., Hargreaves, J. C., Erb, M. P., Emile-Geay, J., D'Agostino, R., Chandan, D., Carré, M., Bartlein, P. J., Zheng, W., Zhang, Z., Zhang, Q., Yang, H., Volodin, E. M., Tomas, R. A., Routson, C., Peltier, W. R., Otto-Bliesner, B., Morozova, P. A., McKay, N. P., Lohmann, G., Legrande, A. N., Guo, C., Cao, J., Brady, E., Annan, J. D., and Abe-Ouchi, A.: Large-scale features and
400 evaluation of the PMIP4-CMIP6 *midHolocene* simulations, Climate of the Past, 16, 1847–1872, https://doi.org/10.5194/cp-16-1847-2020, https://cp.copernicus.org/articles/16/1847/2020/, 2020.

Brown, J. R., Brierley, C. M., An, S.-I., Guarino, M.-V., Stevenson, S., Williams, C. J. R., Zhang, Q., Zhao, A., Abe-Ouchi, A., Braconnot, P., Brady, E. C., Chandan, D., D'Agostino, R., Guo, C., LeGrande, A. N., Lohmann, G., Morozova, P. A., Ohgaito, R., O'ishi, R., Otto-Bliesner, B. L., Peltier, W. R., Shi, X., Sime, L., Volodin, E. M., Zhang, Z., and Zheng, W.: Comparison of past and future simulations
405 of ENSO in CMIP5/PMIP3 and CMIP6/PMIP4 models, Climate of the Past, 16, 1777–1805, https://doi.org/10.5194/cp-16-1777-2020, https://cp.copernicus.org/articles/16/1777/2020/, 2020.

Christensen, J., Krishna Kumar, K., Aldrian, E., An, S.-I., Cavalcanti, I., de Castro, M., Dong, W.and Goswami, P., Hall, A., Kanyanga, J., Kitoh, A., Kossin, J., Lau, N.-C., Renwick, J., Stephenson, D., Xie, S.-P., and Zhou, T.: Climate phenomena and their relevance for future regional climate change, in: Climate change 2013: the physical science basis. Contribution of Working Group I to the Fifth Assessment
410 Report of the Intergovernmental Panel on Climate Change, edited by Stocker, T., Qin, D., Plattner, G.-K., Tignor, M., Allen, S., Boschung, J., Nauels, A., Xia, Y., Bex, V., and Midgley, P., pp. 1217–1308, Cambridge University Press, 2013.

Collins, M., Knutti, R., Arblaster, J., Dufresne, J.-L., Fichefet, T., Friedlingstein, P., Gao, X., Gutowski, W. J., Johns, T., Krinner, G., Shongwe, M., Tebaldi, C., Weaver, A., and Wehner, M.: Long-term climate change: projections, commitments and irreversibility, in: Climate Change 2013-The Physical Science Basis: Contribution of Working Group I to the Fifth Assessment Report of the Intergovernmental Panel on
415 Climate Change, edited by Stocker, T., Qin, D., Plattner, G.-K., Tignor, M., Allen, S., Boschung, J., Nauels, A., Xia, Y., Bex, V., and Midgley, P., pp. 1029–1136, Cambridge University Press, 2013.

Danabasoglu, G., Yeager, S. G., Kwon, Y.-O., Tribbia, J. J., Phillips, A. S., and Hurrell, J. W.: Variability of the Atlantic meridional over-turning circulation in CCSM4, Journal of climate, 25, 5153–5172, 2012.

Douville, H., Raghavan, K., Renwick, J., Allan, R. P., Arias, P. A., Barlow, M., Cerezo-Mota, R., Cherchi, A., Gan, T. Y., Gergis, J., Jiang,
420 D., Khan, A., Pokam Mba, W., Rosenfeld, D., Tierney, J., and Zolina, O.: Water Cycle Changes, in: Climate Change 2021: The Physical Science Basis. Contribution of Working Group I to the Sixth Assessment Report of the Intergovernmental Panel on Climate Change, edited by Masson-Delmotte, V., Zhai, P., Pirani, A., Connors, S. L., Péan, C., Berger, S., Caud, N., Chen, Y., Goldfarb, L., Gomis, M. I., Huang, M., Leitzell, K., Lonnoy, E., Matthews, J., Maycock, T. K., Waterfield, T., Yelekçi, O., Yu, R., , and Zhou, B., Cambridge University Press, 2021.

425 Eyring, V., Bony, S., Meehl, G. A., Senior, C. A., Stevens, B., Stouffer, R. J., and Taylor, K. E.: Overview of the Coupled Model Intercompar-ison Project Phase 6 (CMIP6) experimental design and organization., Geoscientific Model Development, 9, https://doi.org/10.5194/gmd-9-1937-2016, 2016.

Eyring, V., Gillett, N. P., Achuta Rao, K. M., Barimalala, R., Barreiro Parrillo, M., Bellouin, N., Cassou, C., Durack, P. J., Kosaka, Y., McGregor, S., Min, S., Morgenstern, O., and Sun, Y.: Human Influence on the Climate System, in: Climate Change 2021: The Physical

430 Science Basis. Contribution of Working Group I to the Sixth Assessment Report of the Intergovernmental Panel on Climate Change, edited by Masson-Delmotte, V., Zhai, P., Pirani, A., Connors, S. L., Péan, C., Berger, S., Caud, N., Chen, Y., Goldfarb, L., Gomis, M. I., Huang, M., Leitzell, K., Lonnoy, E., Matthews, J., Maycock, T. K., Waterfield, T., Yelekçi, O., Yu, R., , and Zhou, B., Cambridge University Press, 2021.

Fasullo, J. T., Phillips, A., and Deser, C.: Evaluation of leading modes of climate variability in the CMIP archives, Journal of Climate, 33,

435 5527–5545, https://doi.org/10.1175/JCLI-D-19-1024.1, 2020.

Fox-Kemper, B., Hewitt, H. T., Xiao, C., Aðalgeirsdóttir, G., Drijfhout, S. S., Edwards, T. L., Golledge, N. R., Hemer, M., Kopp, R. E., Krinner, G., Mix, A., Notz, D., Nowicki, S., Nurhati, I. S., Ruiz, L., Sallée, J.-B., Slangen, A. B. A., and Yu, Y.: Ocean, Cryosphere and Sea Level Change, in: Climate Change 2021: The Physical Science Basis. Contribution of Working Group I to the Sixth Assessment Report of the Intergovernmental Panel on Climate Change, edited by Masson-Delmotte, V., Zhai, P., Pirani, A., Connors, S. L., Péan, C.,

440 Berger, S., Caud, N., Chen, Y., Goldfarb, L., Gomis, M. I., Huang, M., Leitzell, K., Lonnoy, E., Matthews, J., Maycock, T. K., Waterfield, T., Yelekçi, O., Yu, R., , and Zhou, B., Cambridge University Press, 2021.

Guiterrez, J. M., Iturbide, M., Alvarez, E. C., Diez-Sierra, J., Bedia, J., Manzanas, R., no Medina, J. B., Hauser, M., García-Díez, M., Ozge Yelecki, Felice, M. D., and Trenham, C.: PMIP4-midHolocene, GitHub, https://github.com/IPCC-WG1/Atlas, last access: 12 July 2021, 2021.

445 Gulev, S. K., Thorne, P., Ahn, J., Dentener, F., Domingues, C., Gerland, S., Gong, D., Kaufman, D., Nnamchi, H., Quaas, J., Rivera, J., Sathyendranath, S., Smith, S., Trewin, B., von Shuckmann, K., and Vose, R.: Changing State of the Climate System, in: Climate Change 2021: The Physical Science Basis. Contribution of Working Group I to the Sixth Assessment Report of the Intergovernmental Panel on Climate Change, edited by Masson-Delmotte, V., Zhai, P., Pirani, A., Connors, S. L., Péan, C., Berger, S., Caud, N., Chen, Y., Goldfarb, L., Gomis, M. I., Huang, M., Leitzell, K., Lonnoy, E., Matthews, J., Maycock, T. K., Waterfield, T., Yelekçi, O., Yu, R., , and Zhou, B.,

450 Cambridge University Press, 2021.

Gutiérrez, J. M., Jones, R. G., Narisma, G. T., Alves, L. M., Amjad, M., Gorodetskaya, I. V., Grose, M., Klutse, N. A. B., Krakovska, S., Li, J., Martínez-Castro, D., Mearns, L. O., Mernild, S. H., Ngo-Duc, T., van den Hurk, B., and Yoon, J.-H.: Atlas, in: Climate Change 2021: The Physical Science Basis. Contribution of Working Group I to the Sixth Assessment Report of the Intergovernmental Panel on Climate Change, edited by Masson-Delmotte, V., Zhai, P., Pirani, A., Connors, S. L., Péan, C., Berger, S., Caud, N., Chen, Y., Goldfarb, L., Gomis,

455 M. I., Huang, M., Leitzell, K., Lonnoy, E., Matthews, J., Maycock, T. K., Waterfield, T., Yelekçi, O., Yu, R., , and Zhou, B., Cambridge University Press, 2021.

Harrison, S., Bartlein, P., Brewer, S., Prentice, I., Boyd, M., Hessler, I., Holmgren, K., Izumi, K., and Willis, K.: Climate model benchmarking with glacial and mid-Holocene climates, Climate Dynamics, 43, 671–688, https://doi.org/10.1007/s00382-013-1922-6, 2014.

Harrison, S. P., Bartlein, P., Izumi, K., Li, G., Annan, J., Hargreaves, J., Braconnot, P., and Kageyama, M.: Evaluation of CMIP5 palaeo-

460 simulations to improve climate projections, Nature Climate Change, 5, 735–743, https://doi.org/10.1038/nclimate2649, 2015.

Haywood, A. M., Tindall, J. C., Dowsett, H. J., Dolan, A. M., Foley, K. M., Hunter, S. J., Hill, D. J., Chan, W.-L., Abe-Ouchi, A., Stepanek, C., Lohmann, G., Chandan, D., Peltier, W. R., Tan, N., Contoux, C., Ramstein, G., Li, X., Zhang, Z., Guo, C., Nisancioglu, K. H., Zhang, Q., Li, Q., Kamae, Y., Chandler, M. A., Sohl, L. E., Otto-Bliesner, B. L., Feng, R., Brady, E. C., von der Heydt, A. S., Baatsen, M. L. J., and Lunt, D. J.: The Pliocene Model Intercomparison Project Phase 2: large-scale climate features and climate sensitivity, Climate of the

465 Past, 16, 2095–2123, https://doi.org/10.5194/cp-16-2095-2020, https://cp.copernicus.org/articles/16/2095/2020/, 2020.

Hoyer, S. and Hamman, J.: xarray: N-D labeled arrays and datasets in Python, Journal of Open Research Software, 5, https://doi.org/10.5334/jors.148, http://doi.org/10.5334/jors.148, 2017.

IPCC: Annex V: Monsoons [Cherchi, A., A. Turner (eds.)], in: Climate Change 2021: The Physical Science Basis. Contribution of Working Group I to the Sixth Assessment Report of the Intergovernmental Panel on Climate Change, edited by Masson-Delmotte, V., Zhai, P.,
470   Pirani, A., Connors, S. L., Péan, C., Berger, S., Caud, N., Chen, Y., Goldfarb, L., Gomis, M. I., Huang, M., Leitzell, K., Lonnoy, E., Matthews, J., Maycock, T. K., Waterfield, T., Yelekçi, O., Yu, R., , and Zhou, B., Cambridge University Press, 2021.

Iturbide, M., Gutiérrez, J. M., Alves, L. M., Bedia, J., Cerezo-Mota, R., Cimadevilla, E., Cofiño, A. S., Di Luca, A., Faria, S. H., Gorodet-skaya, I. V., Hauser, M., Herrera, S., Hennessy, K., Hewitt, H. T., Jones, R. G., Krakovska, S., Manzanas, R., Martínez-Castro, D., Narisma, G. T., Nurhati, I. S., Pinto, I., Seneviratne, S. I., van den Hurk, B., and Vera, C. S.: An update of IPCC climate reference re-
475   gions for subcontinental analysis of climate model data: definition and aggregated datasets, Earth System Science Data, 12, 2959–2970, https://doi.org/10.5194/essd-12-2959-2020, https://essd.copernicus.org/articles/12/2959/2020/, 2020.

Juckes, M., Taylor, K. E., Durack, P. J., Lawrence, B., Mizielinski, M. S., Pamment, A., Peterschmitt, J.-Y., Rien, M., and Sénési, S.: The CMIP6 Data Request (DREQ, version 01.00.31), Geoscientific Model Development, 13, 201–224, https://doi.org/10.5194/gmd-13-201-2020, https://gmd.copernicus.org/articles/13/201/2020/, 2020.

480   Kageyama, M., Braconnot, P., Harrison, S. P., Haywood, A. M., Jungclaus, J. H., Otto-Bliesner, B. L., Abe-Ouchi, A., Albani, S., Bartlein, P. J., and Brierley, C.: The PMIP4 contribution to CMIP6-Part 1: Overview and over-arching analysis plan, Geoscientific Model Development, 11, 1033–1057, https://doi.org/10.5194/gmd-11-1033-2018, 2018.

Kageyama, M., Harrison, S. P., Kapsch, M.-L., Lofverstrom, M., Lora, J. M., Mikolajewicz, U., Sherriff-Tadano, S., Vadsaria, T., Abe-Ouchi, A., Bouttes, N., Chandan, D., Gregoire, L. J., Ivanovic, R. F., Izumi, K., LeGrande, A. N., Lhardy, F., Lohmann, G., Morozova, P. A.,
485   Ohgaito, R., Paul, A., Peltier, W. R., Poulsen, C. J., Quiquet, A., Roche, D. M., Shi, X., Tierney, J. E., Valdes, P. J., Volodin, E., and Zhu, J.: The PMIP4 Last Glacial Maximum experiments: preliminary results and comparison with the PMIP3 simulations, Climate of the Past, 17, 1065–1089, https://doi.org/10.5194/cp-17-1065-2021, https://cp.copernicus.org/articles/17/1065/2021/, 2021.

Kitoh, A., Endo, H., Krishna Kumar, K., Cavalcanti, I. F. A., Goswami, P., and Zhou, T.: Monsoons in a chang-ing world: A regional perspective in a global context, Journal of Geophysical Research: Atmospheres, 118, 3053–3065,
490   https://doi.org/https://doi.org/10.1002/jgrd.50258, https://doi.org/10.1002/jgrd.50258, 2013.

Nüst, D., Sochat, V., Marwick, B., Eglen, S. J., Head, T., Hirst, T., and Evans, B. D.: Ten simple rules for writing Dockerfiles for reproducible data science, PLOS Computational Biology, 16, 1–24, https://doi.org/10.1371/journal.pcbi.1008316, https://doi.org/10.1371/journal.pcbi.1008316, 2020.

Otto-Bliesner, B. L., Brady, E. C., Fasullo, J., Jahn, A., Landrum, L., Stevenson, S., Rosenbloom, N., Mai, A., and Strand, G.: Climate
495   variability and change since 850 CE: An ensemble approach with the Community Earth System Model, Bulletin of the American Meteo-rological Society, 97, 735–754, 2016.

Otto-Bliesner, B. L., Braconnot, P., Harrison, S. P., Lunt, D. J., Abe-Ouchi, A., Albani, S., Bartlein, P. J., Capron, E., Carlson, A. E., Dutton, A., et al.: The PMIP4 contribution to CMIP6–Part 2: Two interglacials, scientific objective and experimental design for Holocene and Last Interglacial simulations, Geoscientific Model Development, 10, 3979–4003, https://doi.org/10.5194/gmd-10-3979-2017, 2017.

500   Otto-Bliesner, B. L., Brady, E. C., Zhao, A., Brierley, C. M., Axford, Y., Capron, E., Govin, A., Hoffman, J. S., Isaacs, E., Kageyama, M., Scussolini, P., Tzedakis, P. C., Williams, C. J. R., Wolff, E., Abe-Ouchi, A., Braconnot, P., Ramos Buarque, S., Cao, J., de Vernal, A., Guar-ino, M. V., Guo, C., LeGrande, A. N., Lohmann, G., Meissner, K. J., Menviel, L., Morozova, P. A., Nisancioglu, K. H., O'ishi, R., Salas y Mélia, D., Shi, X., Sicard, M., Sime, L., Stepanek, C., Tomas, R., Volodin, E., Yeung, N. K. H., Zhang, Q., Zhang, Z., and Zheng, W.:

Large-scale features of Last Interglacial climate: results from evaluating the *lig127k* simulations for the Coupled Model Intercomparison Project (CMIP6)–Paleoclimate Modeling Intercomparison Project (PMIP4), Climate of the Past, 17, 63–94, https://doi.org/10.5194/cp-17-63-2021, https://cp.copernicus.org/articles/17/63/2021/, 2021.

Phillips, A. S., Deser, C., and Fasullo, J.: Evaluating modes of variability in climate models, Eos, Transactions American Geophysical Union, 95, 453–455, https://doi.org/10.1002/2014EO490002, 2014.

Pollard, D. and Reusch, D. B.: A calendar conversion method for monthly mean paleoclimate model output with orbital forcing, Journal of Geophysical Research: Atmospheres, 107, 4615–ACL3–7, https://doi.org/10.1029/2002JD002126, 2002.

Rehfeld, K., Hébert, R., Lora, J. M., Lofverstrom, M., and Brierley, C. M.: Variability of surface climate in simulations of past and future, Earth System Dynamics, 11, 447–468, https://doi.org/10.5194/esd-11-447-2020, https://esd.copernicus.org/articles/11/447/2020/, 2020.

Reynolds, R. W., Rayner, N. A., Smith, T. M., Stokes, D. C., and Wang, W.: An Improved In Situ and Satellite SST Analysis for Climate, Journal of Climate, 15, 1609–1625, https://doi.org/10.1175/1520-0442(2002)015<1609:AIISAS>2.0.CO;2, https://journals.ametsoc.org/view/journals/clim/15/13/1520-0442_2002_015_1609_aiisas_2.0.co_2.xml, 2002.

Schmidt, G. A., Annan, J. D., Bartlein, P. J., Cook, B. I., Guilyardi, E., Hargreaves, J. C., Harrison, S. P., Kageyama, M., LeGrande, A. N., Konecky, B., Lovejoy, S., Mann, M. E., Masson-Delmotte, V., Risi, C., Thompson, D., Timmermann, A., Tremblay, L.-B., and Yiou, P.: Using palaeo-climate comparisons to constrain future projections in CMIP5, Climate of the Past, 10, 221–250, https://doi.org/10.5194/cp-10-221-2014, https://www.clim-past.net/10/221/2014/, 2014.

Wang, B. and Ding, Q.: Global monsoon: Dominant mode of annual variation in the tropics, Dynamics of Atmospheres and Oceans, 44, 165–183, https://doi.org/https://doi.org/10.1016/j.dynatmoce.2007.05.002, https://www.sciencedirect.com/science/article/pii/S0377026508000055, current Contributions to Understanding the General Circulation of the Atmosphere Part 2, 2008.

Wang, B., Kim, H.-J., Kikuchi, K., and Kitoh, A.: Diagnostic metrics for evaluation of annual and diurnal cycles, Climate dynamics, 37, 941–955, https://doi.org/10.1007/s00382-010-0877-0, 2011.

Wang, P. X., Wang, B., Cheng, H., Fasullo, J., Guo, Z. T., Kiefer, T., and Liu, Z. Y.: The global monsoon across timescales: coherent variability of regional monsoons, Climate of the Past, 10, 2007–2052, https://doi.org/10.5194/cp-10-2007-2014, https://cp.copernicus.org/articles/10/2007/2014/, 2014.

Zelinka, M. D., Myers, T. A., McCoy, D. T., Po-Chedley, S., Caldwell, P. M., Ceppi, P., Klein, S. A., and Taylor, K. E.: Causes of higher climate sensitivity in CMIP6 models, Geophysical Research Letters, 47, e2019GL085 782, https://doi.org/10.1029/2019GL085782, 2020.

Zender, C. S.: Analysis of self-describing gridded geoscience data with netCDF Operators (NCO), Environmental Modelling & Software, 23, 1338–1342, 2008.